NUMERICAL SIMULATION FOR EVACUATION PROCESS AGAINST TSUNAMI DISASTER AT MIAMI BEACH IN PENANG, MALAYSIA

Muhammad Salleh Abustan[1], Eiji Harada[2] and Hitoshi Gotoh[3]

[1]Graduate School of Engineering, Department of Civil and Earth Resource Engineering, Kyoto University, abustan_msa@yahoo.com.

[2] Department of Civil And Earth Resource Engineering, Kyoto University. harada@particle.kuciv.kyoto-u.ac.jp.

[3] Department of Civil And Earth Resource Engineering, Kyoto University. gotoh@particle.kuciv.kyoto-u.ac.jp.

Quick evacuation from a beach is the key to save lives against tsunami namely, evacuation planning for an appropriate evacuation route and an evacuation place is required. Investigation of an evacuation process by using numerical simulator is regarded to be an efficient measure, because investigation of an evacuation process by an evacuating safety exercise costs us a great deal of effort. In this study, numerical simulations for evacuation process against tsunami at Penang beach in Malaysia have been performed by using the Crowd Behavior Simulator for Disaster Evacuation (CBS-DE), which is based on the Distinct Element Method (DEM) to track individual evacuation behavior in detail. The sequential procedure of evacuation planning with using this kind of evacuation simulator is shown step by step.

Keywords: *DEM, Evacuation analysis, Tsunami, Town planning.*

1. INTRODUCTION

Quick evacuation prior to Tsunami attack is obviously significant. As a precaution, it is necessary to plan an appropriate evacuation route and an evacuation place. By considering the limited information from a safety exercise and a cost-benefit performance, numerical simulation is regarded as an appropriate way for a rational planning. Some points in evacuation route can be crowded due to local concentration due to abrupt inflow of people in a brief time, hence numerical simulator which contains a model of interaction between people is indispensable. Some previous studies utilized the Distinct Element Method (DEM), which employ the mechanical elements for modeling the interaction between people. And applicability of the DEM to the several crowd behavior process have been demonstrated (e.g., Helbing et al., 2000; Park et al., 2004; Kiyono et al., 1996, 1998; Gotoh et al., 2004, 2009). In this study, the computational domain for evacuation planning is the Miami beach in Penang, Malaysia, where the Indian ocean tsunami has caused victims. And the evacuation planning has been performed by using the Crowd Behavior Simulator for Disaster Evacuation (CBS-DE), which is based on the crowd behavior model proposed by Gotoh et al. (2004) to track individual evacuation behavior in detail. The effective evacuation planning has been investigated from the viewpoint of a reduction of time to evacuate.

2. CROWED BEHAVIOR MODEL

(1) Fundamental equations

The present simulator is based on the CBS-DE proposed by Gotoh et al. (2004). The motion of person is written by translational and rotational equations as follows:

$$m_{hi}\dot{\mathbf{v}}_i = \mathbf{F}_{mi} + \mathbf{F}_{ci} \tag{1}$$

$$I_{hi}\dot{\boldsymbol{\omega}}_i = \mathbf{T}_i \tag{2}$$

where m_{hi} is the mass of the person i, $\mathbf{v}_i$ is the velocity of the person i, " $\cdot$ " indicates a time-derivative, $\mathbf{F}_{mi}$ is the autonomous driving force of the person i, $\mathbf{F}_{ci}$ is the interacting force acting on the person i, I_{hi} is the moment of inertia of the person i, $\boldsymbol{\omega}_i$ is the angular velocity of the person i, $\mathbf{T}_i$ is the torque acting on the person i. Each person is modeled as a cylinder element. The mass and the moment of inertia of the person i can be written as:

$$m_{hi} = \varepsilon_{hi}\sigma_{hi}B_{hi}\frac{\pi d_{hi}^{2}}{4} \quad ; \quad I_{hi} = \varepsilon_{hi}\sigma_{hi}B_{hi}\frac{\pi d_{hi}^{4}}{32} \tag{3}$$

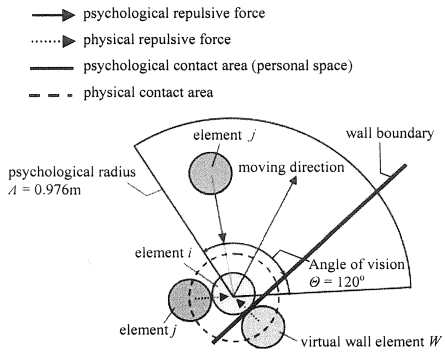

Figure 1: Schematic of perception domain of each person.

where σ_{hi} is the density of the person i, B_{hi} is the body height of the person i, d_{hi} is the diameter of the person element i, ε_{hi} is the correction coefficient concerning the volumetric difference between the cylinder element and the actual person. In the numerical simulation, a positional vector, a velocity vector and an angular velocity are updated explicitly by an Eulerian explicit scheme, and the marching time step Δt is determined with taking care of the numerical stability.

(2) Interacting forces acting on person

With concerning the both physical repulsive force and the psychological repulsive force acting on each person, the perception domain shown in Fig.1 is applied. This perception domain is symmetric to the moving direction of each person. The physical repulsive force acts when two adjacent person elements i and j, or person i and the virtual wall element satisfy the following conditions, respectively:

$$\left|\mathbf{r}_i - \mathbf{r}_j\right| \le \frac{d_{hi} + d_{hj}}{2} \quad ; \quad \left|\mathbf{r}_i - \mathbf{r}_W\right| \le \frac{d_{hi} + d_W}{2} \qquad (4)$$

where $\mathbf{r}_i$ is the positional vector of the person i, $\mathbf{r}_W$ is the positional vector of the virtual wall element W, d_W is the diameter of the virtual wall element W. The virtual wall element is located on the wall having tangential contact with the person i.

The psychological repulsive force acts when two adjacent persons i and j satisfy the following condition:

$$\left|\mathbf{r}_i - \mathbf{r}_j\right| \le \Lambda \qquad (5)$$

where Λ is psychological radius. The perception domain of the psychological repulsive force is determined by considering both the angle of vision Θ (=120 degrees) and the psychological radius Λ.

The psychological radius is interpreted as the representative length scale of a personal space. In the present study, we employ the psychological radius as the averaged relative distance between pedestrians stopping at a red light, which was observed by Kiyono et. al.(1996). Both the physical repulsive force and the psychological repulsive force are estimated by the Voigt model (spring-dashpot system). Note that the physical repulsive force acts between person and between the person and wall, meanwhile, the psychological repulsive force acts only between persons. And the wall repulsive force is exerted on the person by the virtual wall element W, located on the wall having tangential contact with the person. The total force acting on the person i is described as follows:

$$\mathbf{F}_{ci} = \mathbf{F}_{d(p/p)i} + \mathbf{F}_{d(W/p)i} + \mathbf{F}_{ps\ i} \qquad (6)$$

$$\mathbf{F}_{d(p/p)i} = \sum_{j(\neq i)} \mathbf{f}_{ij} \quad ; \quad \mathbf{F}_{d(W/p)i} = \sum_{j(\neq i)} \mathbf{f}_{iW} \quad ; \quad \mathbf{F}_{ps\ i} = \sum_{j(\neq i)} \mathbf{f}_{ps\ Ij} \qquad (7)$$

$$\mathbf{T}_i = \frac{1}{2}\left\{ \sum_{j(\neq i)} (\mathbf{r}_j - \mathbf{r}_i) \times \mathbf{f}_{ij} + \sum_{W} (\mathbf{r}_W - \mathbf{r}_i) \times \mathbf{f}_{iW} \right\} \qquad (8)$$

where $\mathbf{F}_{d(p/p)i}$ is the physical repulsive force acting on the person i, $\mathbf{F}_{d(W/p)i}$ is the physical repulsive force between the virtual wall element W and the person i, $\mathbf{F}_{ps\ i}$ is the psychological repulsive force acting on the person i, $\mathbf{f}_{ij}$ is the local physical repulsive force between the persons i and j, $\mathbf{f}_{iW}$ is the local physical repulsive force between the person i and the virtual wall element W, $\mathbf{f}_{ps\ ij}$ is the local psychological repulsive force between the persons i and j. These local repulsive forces $\mathbf{f}_{ij}$, $\mathbf{f}_{iW}$ and $\mathbf{f}_{ps\ ij}$ are given as follows:

$$\mathbf{f}_{com.} = \left[\frac{\left(\mathbf{e}^n\right)^{pre} + k^n \Delta r^n \mathbf{n}}{\mathbf{e}^n} + \frac{c^n \Delta v^n \mathbf{n}}{\mathbf{d}^n} \right]_{com.} + \left[\frac{\left(\mathbf{e}^t\right)^{pre} + k^t \Delta r^t \mathbf{t}}{\mathbf{e}^t} + \frac{c^t \Delta v^n \mathbf{t}}{\mathbf{d}^n} \right]_{com.} = \mathbf{f}^n + \mathbf{f}^t \qquad (9)$$

$$\mathbf{f}^n = \mathbf{e}^n + \mathbf{d}^n \quad ; \quad \mathbf{f}^t = \mathbf{e}^t + \mathbf{d}^t$$

$$\Delta r^n = [\mathbf{r}_{target} - \mathbf{r}_i]_{\Delta t} \cdot \mathbf{n} \; ; \; \Delta r^t = [\mathbf{r}_{target} - \mathbf{r}_i]_{\Delta t} \cdot \mathbf{t} \; ; \; d = |\mathbf{r}_i - \mathbf{r}_{target}|$$

$$\mathbf{n} = (\mathbf{r}_i - \mathbf{r}_{target})/d = (n^1, n^2) \; ; \; \mathbf{t} = (-n^2, n^1) \qquad (10)$$

$$\Delta v^n = (\mathbf{v}_{target} - \mathbf{v}_i) \cdot \mathbf{n} \; ; \; \Delta v^t = (\mathbf{v}_{target} - \mathbf{v}_i) \cdot \mathbf{t}$$

where $\mathbf{e}^n$ and $\mathbf{e}^t$ denote the component of the repulsive force due to the elastic springs, the spring constants of which are k^n and k^t in the normal and

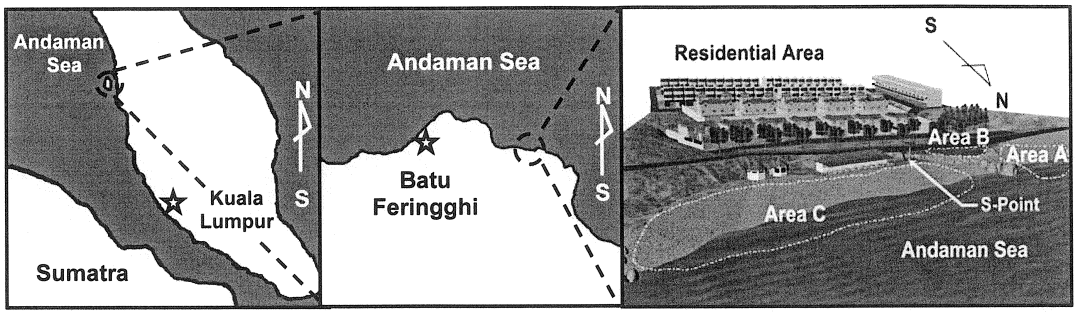

Figure 2: Top and perspective view of Miami Beach.

the tangential directions, respectively, $\mathbf{d}^n$ and $\mathbf{d}^t$ denote the component of the repulsive force due to the viscosity dashpots, the dashpot constants of which are c^n and c^t in the normal and tangential directions, respectively, $\mathbf{f}^n$ and $\mathbf{f}^t$ are the total repulsive force in the normal and tangential directions, respectively. The superscript "*pre*" indicates the previous numerical time step, $\mathbf{r}_{target}$ represents the positional vector of the target element. Subscript "*com.*" indicates *ij*, *iW* and *ps ij*, and the corresponding the subscript "*target*" are the person *j* and the virtual wall element *W*.

In the present simulation, we do not consider a special attractive force between flocks, such as a family, friends and a couple. To simulate a flock behavior, a psychological attractive force between persons should be incorporated. Here, we assumed that each person walks independently without any special psychological attractive force. Hence the joint without resistance against tensile force is allocated in the normal direction as follows:

$$\mathbf{f}_{com.} = 0.0 \ then \ \mathbf{e}^n < 0.0 \qquad (11)$$

Meanwhile, the frictional force works in the tangential direction as follows:

$$|\mathbf{e}^t| > \mu \mathbf{e}^n \text{ then } \mathbf{f}^t = \mu \cdot \text{SIGN}(\mathbf{e}^n, \mathbf{e}^t) \qquad (12)$$

$$\text{SIGN}(a,b) = \begin{cases} |a| \ when \ b \geq 0 \\ -|a| \ when \ b < 0 \end{cases} \qquad (13)$$

where μ is the frictional coefficient at the contact point.

(3) Autonomous driving force

Each isolated person is assumed to be able to walk in the specific equilibrium velocity. When a person experiences a loss of velocity, person is uniformly accelerated by the autonomous driving force $\mathbf{F}_{mi}$ as follows:

$$\mathbf{F}_{mi} = m_i \mathbf{a} \qquad (14)$$

where $\mathbf{a}$ is the acceleration vector. The equilibrium

Table 1: Detail population in Miami beach (above); Initial arrangement of people in each area (below).

Category	Gender	Age	Number	Ratio	Velocity (m/s)
1	Male	10-39	93	27.93	1.45
2	Male	40-69	53	15.92	1.19
3	Male	Over 70	4	1.20	0.99
4	Female	10-39	93	27.93	1.23
5	Female	40-69	41	12.31	1.04
6	Female	Over 70	3	0.90	0.89
7	Child	5-9	46	13.81	1.06
		Total	333	100%	

Area	Category							Total
	1	2	3	4	5	6	7	
A	30	22	2	32	12	1	17	116
B	9	6	-	9	6	1	3	34
C	52	25	2	53	23	1	27	184

velocity is influenced by the number density of persons. A linear correlation between the number density of persons and the equilibrium velocity was observed by Liu et al. (2008). Therefore, the magnitude of the maximum equilibrium velocity v_{max} is written as follows:

$$v_{max} = v_{limit} - \gamma \cdot c_k \qquad (15)$$

where γ is the proportional coefficient, v_{limit} is the magnitude of the specific equilibrium velocity in an isolated walking condition, c_k is the number density of persons inside the psychological perception area (See Fig.1). The specific equilibrium velocity v_{limit} and the coefficient γ are tuned by the observation results.

(4) Model constants

The physical normal spring constant k^n ($=1.26\times10^4$ N/m) between persons was measured by Kiyono et al. (1998) with compressing actual human body. The physical normal spring constant between person and wall was assumed to be twice as much as that of between persons because a wall is a fixed boundary. And the psychological normal spring constant k^n between persons is determined by setting autonomous driving force, which is equal to

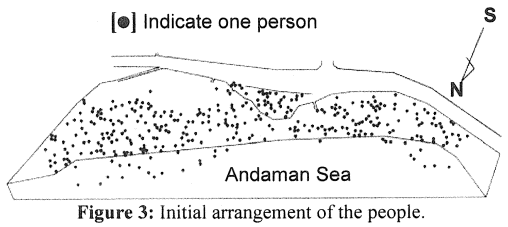

Figure 3: Initial arrangement of the people.

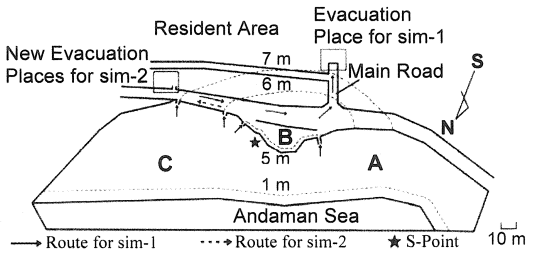

Figure 4: Evacuation route in sim-1 and sim-2 for divided sub-domain A, B, C.

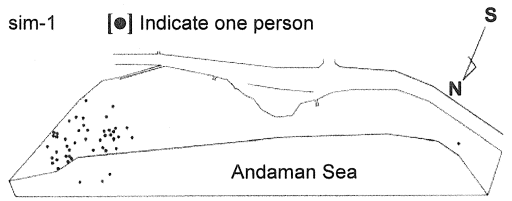

Figure 5: Default position of peoples who need more than 250 seconds for the completion of evacuation.

the normal component of the psychological force under the minimum psychological distance between persons. Meanwhile, the normal viscosity constant is set to satisfy the critical damping condition of the Voigt model in a single degree of freedom. And the tangential dashpot constant which is 0.05 times as much as the normal dashpot constant is applied by referring to Kiyono et al.(1996).

3. RESULTS AND DISCUSSION

(1) Simulation set up

In this study, Miami Beach of Penang Island, where thousands of tourists visit every year and a lot of people have suffered from Indian ocean tsunami, is selected as the site for simulating an evacuation process. Fig. 2 shows the computational domain around Miami Beach which is located in sea-front delta with a hill on its back.

The height of the hill is approximately 23 meters above the sea level and it has an adequate height for an evacuation place against tsunami. According to the field surveys, the peak distribution of population in Miami beach is shown in Tab. 1 (above) and people are arranged at random as the

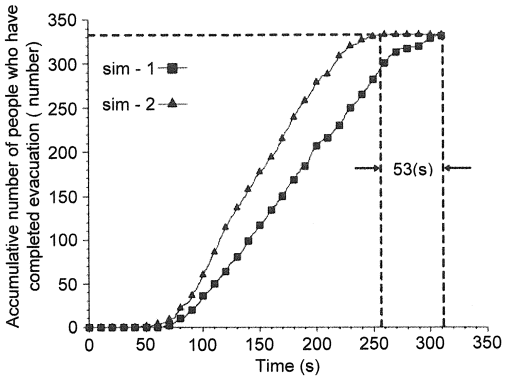

Figure 6: Time series of the accumulative number of people who have completed evacuation of sim-1 and sim-2, respectively.

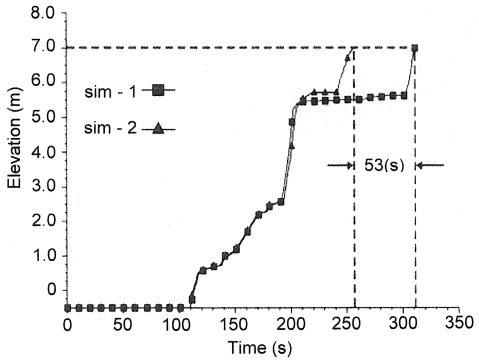

Figure 7: Time series of attained minimum elevation above sea level for all people.

initial condition in three sub-domains as shown in Tab. 1(below). Most of visitors were between the age of 10 and 39 in both male and female. The equilibrium velocity shown in Tab. 1(above) was given by Gotoh et al. (2004). In the present simulation, the completion of evacuation is assumed that all people reach at altitude of more than 7 meters above the sea level, which is based on the observed tsunami record in 2004. We assumed the condition that the warning device breaks down and people begin an evacuation process after receiving the verbal evacuation signal propagated concentrically from the S-point shown in Fig. 2. And the speed of the propagation of the evacuation signal is set as 1.5m/s.

(2) Investigation of present condition for evacuation

For the first step of the process of the evacuation planning, the simulation, in which the evacuation place is designated in the end of the main road which leads from coast as shown in Fig. 4, has been performed as the sim-1. And the disadvantageous area to quick evacuation has been revealed. Fig. 3

shows the initial arrangement of the people who are arranged at random in the coast. Fig. 4 shows the evacuation route to reach the evacuation place in the sim-1. All the people evacuate toward the designated evacuation place. The distribution of the initial arrangement of the people who cannot evacuate within 250 seconds is shown in Fig. 5. The number of the people who cannot evacuate within 250 seconds is estimated to be 47 and the area where delay in evacuation is detected in the east end of the area-C.

(3) Effect of additional evacuation place

To evacuate smoothly person who is in the disadvantageous area, another scenario has been investigated in the sim-2 from the viewpoint of efficient evacuation. The initial arrangement of the people in the sim-2 is the same as that of sim-1. Fig. 4 also shows the evacuation route of the sim-2, in which the dashed arrow shows the difference from the route of sim-1. In the sim-2, people arranged in the area-C are specified to evacuate to the new evacuation place around the east end of the residential area as shown in Fig.2. To investigate the differences of the evacuation processes between sim-1 and sim-2 particularly, the time series of the accumulative number of people who have completed evacuation is shown in Fig. 6. The efficiency of evacuation of the sim-2 is found to be higher than that of sim-1. A decrease in the time of the completion of the evacuation of the sim-2 is 53 seconds in comparison to that of the sim-1. Fig. 7 shows the time series of minimum attain elevation of all the people. The difference between sim-1 and sim-2 in the time series is found to be slight until the minimum attain elevation is about 5 meters. And it is shown that the drastic difference appears in the evacuation process between from 5 to 7 meters. From these results, the reduction of time of the completion of the evacuation is found and the effect of the additional evacuation place is confirmed in the sim-2.

4. CONCLUSION

In this study, the process of the evacuation planning has been shown through the numerical simulation for the evacuation against tsunami at Miami beach at Penang, Malaysia by using the Crowd Behavior Simulator for Disaster Evacuation (CBS-DE) based on the distinct element method. In the process of the evacuation planning, the disadvantageous area has been revealed firstly, then the alternative planning for the improvement of the

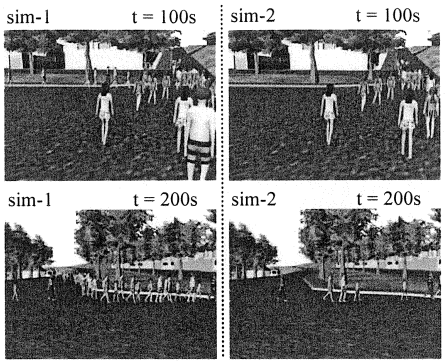

Figure 8: Typical CG snapshots of simulation sim-1 and sim-2 during evacuation process.

disadvantageous area has been investigated, and the effect of the alternative planning has been shown quantitatively. Simulation results provides us the behavior of each person in detail, so we can create a virtual space by CG as shown in Fig. 8. This kind of the CG will be considered to be a useful tool for explaining the evacuation planning to the public.

REFERENCES

Gotoh, H., Harada, E., Kubo, Y., and Sakai, T. (2004): Particle-System Model of the behavior of Crowd in Tsunami Flood Refuge, *Annual Jour. Of Coastal Engineering, JSCE,* Vol.51, pp.1261-1265 (in Japanase).

Gotoh, H., Harada, E., and Ohniwa, K. (2009): Numerical Simulation of Coastal Town Planning against Tsunami by DEM-base Human Behavior Simulator, *Proceeding of the Nineteenth (2009) International Offshore and Polar Engineering Conference,* Osaka, Japan, pp.1248-1252.

Helbing, D., Farkas, I., and Vicsek, T. (2000): Simulating dynamical features of escape panic, *Nature* 407, pp.487–490.

Kiyono, J., Miura, F., and Takimoto, K. (1996): Simulation of emergency evacuation behaviour during disaster by using distinct element method, *Journal of structural mechanics and earthquake engineering, JSCE,* 591(I-43), pp.365-378 (in Japanese).

Kiyono, J., Miura, F., Yagi, H., (1998): Simulation of evacuation behavior in a disaster by distinct element method, *Journal of structural mechanics and earthquake engineering, JSCE,* 591(I-43), pp.365-378 (in Japanese).

Liu, Chien-Hung, Ooeda, Y., and Sumi, T. (2008): A model for pedestrian movement with obstacle evasion using personal space concept, *Dboku Gakkai Ronbunshuu D,* Vol.64, No.4, pp.513-524 (in Japanese)

Park, J., Lee, D., Kim, H., and Yang, Y. (2004): Development of evacuation model for human safety in maritime casualty. *Ocean Engineering* 31, pp.1537-1547.

Smith, A., James, C., Jones, R., Langston, P., Lester, E., and Drury, J. (2009): Modeling contra-flow in crowd dynamics DEM simulation, *Safety Science* 47(3), pp.395-404.

(Received March 18, 2011)